Robust satellite techniques for remote sensing of seismically active areas

Valerio Tramutoli ([1]), **Gerardo Di Bello** ([1]), **Nicola Pergola** ([2]) **and Sabatino Piscitelli** ([2])
([1]) *Dipartimento di Ingegneria e Fisica dell'Ambiente, Università della Basilicata, Potenza, Italy*
([2]) *Istituto di Metodologie Avanzate di Analisi Ambientale, CNR, Potenza, Italy*

Abstract
Several satellite techniques have been recently proposed to remotely map seismically active zones and to monitor geophysical phenomena possibly associated with earthquakes. Even if questionable in terms of their effective applicability, all these techniques highlight as the major problem, still to be overcome, the high number of natural factors (independent of any seismic activity) whose variable contributions to the investigated signal can be so high as to completely mask (or simulate) the space-time anomaly possibly associated to the seismic event under study. A robust approach (RAT) has recently been proposed (and successfully applied in the field of the monitoring of the major environmental risks) which, better than other methods, seems suitable for recognising space-time anomalies in the satellite observational field also in the presence of highly variable contributions from atmospheric (transmittance), surface (emissivity and morphology) and observational (time/season, but also solar and satellite zenithal angles) conditions.This work presents the first preliminary results, based on several years of NOAA/AVHRR observations, regarding its extension to satellite monitoring of thermal anomalies possibly associated to seismically active areas of Southern Italy. The main merits of this approach are its robustness against the possibility of false events detection (specially important for this kind of applications) as well as its intrinsic exportability not only to different geographic areas but also to different satellite instrumental packages.

Key words *earthquakes – satellite remote sensing – thermal IR anomaly – robust satellite techniques – seismogenic areas monitoring*

1. Introduction

Several studies have done, suggesting on the basis of satellite and ground-based observations that space-time anomalies in the Thermal Infrared (TIR) radiances fields measured by satellite can be related to seismogenic areas distribution, as well as to their activation before earthquakes. The commonly accepted explanation of this correlation (see, for instance, Qiang Zu-ji *et al*, 1991, as well as the arguments proposed by Tronin, 1996, against other explanatory models) relies on the following, simplified, considerations.

a) Earth degassing activity is expected:
i) to be generally more intense alongside seismogenic faults (spatially stable anomalies);
ii) to increase in the pre-seismic phase as far as the process of micro-cracks extensive formation proceeds under a continuously increasing stress field (space-time non-stable anomalies);
iii) to invert this trend as soon as the stress field becomes locally so high to close the cracks and earthquake occurrence is approaching (Qiang Zu-ji *et al.*, 1991).

b) Anomalous concentration of optically active gases (such as CO_2, CH_4, etc.) in near-surface atmospheric layers, consequent to Earth

Mailing address: Dr. Valerio Tramutoli, Dipartimento di Ingegneria e Fisica dell'Ambiente, Università della Basilicata, Via della Tecnica 3, 85100 Potenza, Italy; e-mail: tramutoli@unibas.it

degassing activity, results in a local greenhouse effect increasing ground temperature.

c) As the TIR radiation received by satellites, in the 8-14 μm atmospheric window, is mainly related to the ground temperature, Earth degassing activity can be monitored, in the space-time domain, by satellite TIR surveys.

Thanks to the direct correlation between degassing intensity, ground temperature and TIR emission, all implications (a), (b) and (c) of Earth degassing intensity and spatial distribution on seismic activities should be applicable to the intensity and spatial distribution of the TIR signal received by satellite.

Observational and theoretical arguments have been proposed to support the above-mentioned relations between greenhouse gases (and particularly CO_2) discharges and seismogenic zones distribution (*e.g.*, Irwin and Barnes, 1980), as well as between earthquakes preparatory phenomena and their occurrence (Scholz *et al.*, 1973).

Several satellite TIR surveys and ground-based observations are claimed to support the relations of TIR anomalies and earthquakes. Qiang Zu-ji *et al.* (1991), on the basis of Meteosat observations, report TIR anomalies, associated with anomalous values (up to 1000-1500 ppm) of emitted greenhouse gases (mainly CO_2, H_2, H_2O), few days before the Datong earthquake (18 October 1989, $M_S = 6.1$) with a period of quiescence just one-day before the event. A few days before the Changsu event (9 February 1990, $M_S = 5.1$), Meteosat TIR anomalies were observed (Qiang Zu-ji *et al.*, 1992a) in combination with an anomalous air temperature increase from the earth surface up to the altitude of 5.5 km (with a maximum increase around 1.5 km). By using AVHRR (Advanced Very High Resolution Radiometer on board NOAA satellites), Wang and Zhu (1984) report TIR observations corresponding to soil surface temperature anomalies, up to 2.5°C, in the zone of preparation of the 1976 Tanghsan earthquake ($M_S > 7$). Qiang Zu-ji *et al.* (1992b) report AVHRR TIR anomalies observed a few days before the Gonghe earthquake (26 April 1990, $M_S = 7.0$) over an area up to 10^6 km^2. The same authors assert that 11 among 15 earthquakes of magnitude greater than 5.1 occurring in China in 1989 had similar pre-event anomalies (the remaining four events all occurred in the Tibet plateau in association with highly variable meteorological factors). Tronin (1996) finds AVHRR TIR anomalies in a statistically significant spatial correlation with Central Asian seismoactive zones. He notes also that TIR anomalies increase their spatial extension (but not intensity) in significant temporal relation to the seismic activation of the Tien Shan and Turan plates in the point of intersection of major crust faults (Karatau and Tamdy-Tokraus).

Such relations of TIR anomalies with seismic activity have been considered with some prudence by the scientific community up to now (see for instance the comments of the sub-commission on Earthquake Prediction at the recent IASPEI meeting) mainly for the insufficiency of the validation data-sets and the scarce importance attached to other causes (*e.g.*, meteorological) that could be responsible for the observed TIR anomalies rather than seismic activity. Actually, a clear definition of *TIR anomaly* as well as a clear description of the satellite data processing phases which could isolate TIR anomalies connected with seismic activities from any other cause, is very hard to find in the above papers.

This is a not trivial problem, as satellite TIR radiances strongly depend on a number of natural (*e.g.*, atmospheric transmittance, surface emissivity and topography) and observational (time/season, but also solar and satellite zenithal angles) conditions, whose variable contributions to the investigated signal can be so high to completely mask (or simulate) the space-time anomaly possibly associated to the seismic event under study.

A robust approach (Tramutoli, 1998) has recently been proposed (and successfully applied in the field of the monitoring of the major environmental risks) which seems suitable for recognising space-time anomalies in the satellite observational field, also in the presence of highly variable natural and observational conditions. In this paper we present the result of a preliminary study, based on several years (from 1980 to 1999) of AVHRR observations, devoted to verifying the existence of space-time relations between thermal anomalies and seismic activity in Southern Italy.

2. Thermal anomaly definition

A sequence of satellite imagery can be represented by a (spectral) *space-time process* giving the radiance $R_{\Delta\lambda}(\boldsymbol{r},t)$, collected in correspondence of a location centered on the ground coordinates $\boldsymbol{r} \equiv (x, y)$ at time t, in the spectral band $\Delta\lambda$. For each fixed location $\boldsymbol{r} = \boldsymbol{r}'$ the quantity $R_{\Delta\lambda}(\boldsymbol{r}', t)$ represents a *time-series*. A satellite image collected, at a fixed time $t = t'$, in the spectral band $\Delta\lambda$, can be then represented by a *purely spatial process* $R_{\Delta\lambda}(\boldsymbol{r}',t')$. A single satellite sounding referred to a fixed location $\boldsymbol{r}'$ and time t' is a *punctual process* $R_{\Delta\lambda}(\boldsymbol{r}',t')$ in the space-time domain.

Thermal infrared radiance, $R_{\mathrm{TIR}}(\boldsymbol{r}, t)$, measured from satellite (usually given in terms of Brightness Temperatures, BT) at the time t, within the TIR, 8-14 μm, atmospheric window, depends on observational (time t of the day and of the year, satellite zenithal angle θ_{SAT}) and physical conditions of Earth surface (mainly temperature T_S and spectral emissivity $\varepsilon_{\mathrm{TIR}}$) and atmosphere (mainly spectral transmittance $\Im_{\mathrm{TIR}}$)

$$R_{\mathrm{TIR}}(\boldsymbol{r},t) = f[\varepsilon_{\mathrm{TIR}}(\boldsymbol{r},t), \Im_{\mathrm{TIR}}(\boldsymbol{r},t), T_S(\boldsymbol{r},t), \theta_{\mathrm{SAT}}(\boldsymbol{r},t)]. \tag{2.1}$$

By separately considering each contribution it must be noted that:

a) Spectral emissivity, which strongly influences TIR signal (variations in the estimate of land surface temperature from 1 to 3°C are expected as a consequence of uncertainty on the emissivity of only $\Delta\varepsilon_{\mathrm{TIR}} \approx 0.01$, *e.g.*, Becker, 1987) takes values within 0.90 and 0.98 over land, mainly depending on soil cover (from bare up to highly vegetated) and humidity.

b) Spectral transmittance depends mainly on atmospheric temperature and humidity vertical profiles and can be assumed weakly variable in the spatial domain only in very stable meteorological conditions.

c) Temporal variations of surface temperature are obviously related to the regular daily and yearly solar cycles but sensitive also to meteorological (climatological) factors leading considerable local variations within one day (one year) and another. Surface temperature spatially depends on local geographical (altitude above sea level, solar exposition, geographic latitude) and physical factors (thermal inertia, albedo, emissivity, etc...).

d) Variations in observational conditions, related mainly to differences in satellite zenithal angles (with consequent reduction of both spatial resolution and measured TIR signal in off-nadir views), introduce systematic spatial variations of the registered signal not related to real near surface thermal discontinuities.

e) For instrumental packages on board polar satellites like NOAA (and differently from geostationary platforms) the same location is observed, at each revisiting time, at different satellite zenithal angle introducing, even assuming a perfect image-to-image co-location, a spurious temporal variation of the measured signal due simply to the change in observational conditions.

f) A perfect image-to-image co-location is impossible (due to the change in the size of each ground resolution cell consequent to the change in the satellite angle of view) so that a spurious temporal variation of the measured signal can be observed as a consequence not only of a residual co-location error, but also because of the change in the size of the ground resolution cell.

At least these aspects should be considered, and their individual contributions to space-time variability of the observed TIR signal evaluated, as a *natural/observational noise*, in order to define space-time TIR anomalies in the context of seismogenic areas monitoring by satellites.

As an example, variations greater than 5 K in the NOAA-AVHRR channel 4 Brightness Temperature (hereafter T_4) can be easily observed as a consequence of the change of one only of the above mentioned natural/observational factors. This noise can then be as large as (in some cases greater than) the TIR signal variations reported in literature as thermal anomalies and attributed to seismogenic activities.

In this context, it is quite obvious that we can assume as anomalous only those signal variations not related to the *normal* (*i.e.* independent of any variation in seismogenic areas distribution and/or activation) space-time variability of the signal itself.

Particularly important becomes then the preliminary definition of this *normal* behaviour of the TIR signal. In fact as both experience and common sense teach, *no signal can be interpreted as anomalous «in se» but only by comparison* with a normality which must be preliminarily defined. On the other hand, it is obvious that *the same signal, which is normally observable at a specific time and place, could appear to be anomalous when observed in a different time and place*. Therefore suitable criteria for space/time anomaly-detection should take into account the *normal* space/time variability of the observable with reference to the specific time t and place $\boldsymbol{r}$ of the observation.

3. A robust approach for satellite thermal anomalies monitoring in seismoactive regions

According to the approach suggested by Tramutoli (1998) and to define the *normal* behaviour of both the TIR signal and its variation in the space-time domain, the following steps have been performed:

1) *Imagery selection*: only AVHRR imagery from 1978 up to 1998 collected in the same month of the year (November) around the same (local) time of day (6:00 PM) was considered as a potential reference data set. Effects related to yearly and daily cycles are therefore reduced. Moreover, late afternoon imagery is less influenced by effects related to soil-air temperature differences, normally higher during other hours of the day, and less sensitive to local solar exposition. This step corresponds to the prescriptions on the *temporal support* (Tramutoli, 1998) T which defines satellite passes to be included in the following processing steps, on the basis of their acquisition time $t \in T$.

2) *Imagery pre-processing*: for each AVHRR scene radiometric calibration was performed, following Lauritson *et al.* (1979) and brightness temperature T_4 in the TIR AVHRR channel 4 (10.3-11.3 μm, the last influenced by space-time variation in atmospheric water vapour content) saved for the following steps with the exclusion of all cloudy soundings (detected by using standard threshold tests on AVHRR IR channels).

3) *Imagery co-location*: all images were accurately geo-referenced (using the automated procedure proposed by Pergola and Tramutoli, 2000), co-located and re-mapped in the same geographic projection (Lambert Azimuthal Equal Area with Nearest Neighbour resampling) in order to build the $T_4(\boldsymbol{r},t)$ reference data set. All soundings over sea were excluded at this stage from the following steps.

4) *Reducing climatological effects*: for each scene the (spatial) average $T_4(t')$ of $T_4(\boldsymbol{r},t')$ and its standard deviation $\sigma_{T4}(t')$ were computed and the quantity $\Delta T_4(\boldsymbol{r},t') = T_4(\boldsymbol{r},t') - T_4(t')$ saved for the following steps. The use of spatial averages, to take into account the year-to-year variation in the temperature field, will increase in efficiency the larger the area considered with respect to the expected extension of thermal anomalies and the more representative of different temperature regimes (mainly related to altitude) and soil emissivities (depending on soil cover properties and particularly on vegetation). In this way, the observable to be used will no longer be the *llocal* (using hereafter the double *l* introduced by Tramutoli, 1998, to indicate a punctual value in the space and time domain) value of the absolute brightness temperature $T_4(\boldsymbol{r}',t')$ measured at the time t' and place $\boldsymbol{r}'$, but its *llocal* excess with respect to the value $T_4(t')$ assumed as representative of the normal trend of the temperature field on the area at the observation time t'. This, in principle, will permit us to compare values assumed by the observable $\Delta T_4(\boldsymbol{r},t')$ (which completely preserves, as $\sigma\Delta_{T4}(t') = \sigma_{T4}(t')$, the spatial dynamics of $T_4(\boldsymbol{r}',t')$ across the scene) in different years having different climatological temperature trends.

In our case, only land locations within an area (D) of about 600×600 km around the main epicentral zone of the Irpinia-Basilicata earthquake (23 November 1980, $M_S = 6.9$) were considered to which we will refer, hereafter, simply by the word «scene» ($\boldsymbol{r} \in D$, are then the prescriptions on the *spatial support*, requested in Tramutoli (1998), which defines the spatial domain and arrangement of sites to be processed).

5) *Characterising the* $\Delta T_4(\boldsymbol{r},t)$ *signal in the time domain*: for each land location $\boldsymbol{r} = \boldsymbol{r}'$ the time average $<\Delta T_4(\boldsymbol{r}')>$ and standard deviation

$\sigma_{\Delta T4}(r')$ were computed. These quantities refer to the time-series built for the location r' using (see step 1) observations taken in *llocal* conditions as similar as possible (same hour of the day and month of the year, same altitude, similar soil cover). They include, moreover, all residual uncertainties due to the known and unknown sources of *llocal* signal variability (*e.g.*, changes in atmospheric transmittance, soil humidity, observational view angles, navigation and co-location inaccuracies, etc.).

6) *Index of spatial anomaly definition*: the quantity

$$\otimes^{s}(r,t') \equiv \frac{[\Delta T_4(r,t') - <\Delta T_4(r)>]}{\sigma_{\Delta T4}(t')} \qquad (3.1)$$

gives the *llocal* excess of $\Delta T_4(r,t')$ compared with its historical mean value at the considered location weighted by the present (at the time $t = t'$) variability of the T_4 signal across the scene.

7) *Index of temporal anomaly definition*: the quantity

$$\otimes^{t}(r,t') \equiv \frac{[\Delta T_4(r,t') - <\Delta T_4(r)>]}{\sigma_{\Delta T4}(r)} \qquad (3.2)$$

gives the *llocal* excess of $\Delta T_4(r,t)$ compared with its historical mean value (and weighted by its historical variability) at the considered location.

The indices (3.1) and (3.2) belong to the ALICE (Absolutely Llocal Index of Change of the Environment) class of robust, change detection indices, specifically introduced by Tramutoli (1998) for satellite applications in the field of environmental processes monitoring. They are all determined on the basis of satellite data at hands. From this a number of relevant characteristics descend:

a) No ancillary data (*e.g.*, ground observations) are required, so that their computation can be completely automated for operational real-time monitoring purposes. For the same reason, they are intrinsically exportable to different satellite packages and different geographic areas.

b) They strongly reduce (as explained previously) the effects of known sources of natural/observational noise, but take into account (by means of the denominator term) the effects of the residual noise due to non-predictable signal variability related to *llocal* atmospheric and earth surface conditions (*e.g.*, change in soil and atmospheric moisture).

c) By including the maximum of possible residual noise they are intrinsically resistant to false alarms proliferation (which means, on the other hand, that the signal to be detected must be strong enough to stand out with respect to the remaining natural and observational noise).

All these aspects were evaluated by applying the above procedure to the Irpinia-Basilicata earthquake (23 November 1980, $M_S = 6.9$) using only NOAA-AVHRR observations collected in November from 1980 up to 1999.

4. The investigated area and the Irpinia-Basilicata earthquake (23 November 1980, $M_S = 6.9$)

Southern Italy is one of the most active areas of the Mediterranean region. It is commonly accepted that the largest historical and recent earthquakes which occurred in this area, are typically generated by main normal faults running parallel to the Apennines, while moderate earthquakes are produced by secondary transverse strike-slip faults. Figure 1a shows the locations of the main seismogenic faults, together with the thermically anomalous ($T > 17$°C) source springs, recognised all over the considered area (*e.g.*, Valensise *et al.*, 1993; Boschi *et al.*, 1995, http://faust.ingv.it; Albarello and Martinelli, 1997).

In particular, concerning the Irpinia-Basilicata area, three events with $M_S \sim 7.0$ (1694, 1930 and 1980) occurred in the last four centuries. The November 23, 1980 normal-faulting earthquake ($M_S = 6.9$; seismic moment $M_0 = 26 \times 10^{18}$ Nm) was one of the largest events observed in the Southern Apennines in this century (Westaway and Jackson, 1987; Bernard and Zollo, 1989; Pantosti and Valensise, 1990; Amato and Selvaggi, 1993). It was the first well-

documented example of surface faulting in the Italian peninsula. The seismological analysis revealed that the event was characterised by at least three different rupture episodes occurring at 0 s, ~ 20 s and ~ 40 s. The aftershocks were concentrated within 15 km depth (similarly to the other well-determined focal depths in Central and Southern Apennines) outlining a fault extending approximately 40 km (see for instance Amato and Selvaggi, 1993). For this area, Pantosti and Valensise (1990) hypothesise the existence of a «characteristic earthquake» with M_S ~ 7.0 that releases completely the deformation energy of the area, without producing a

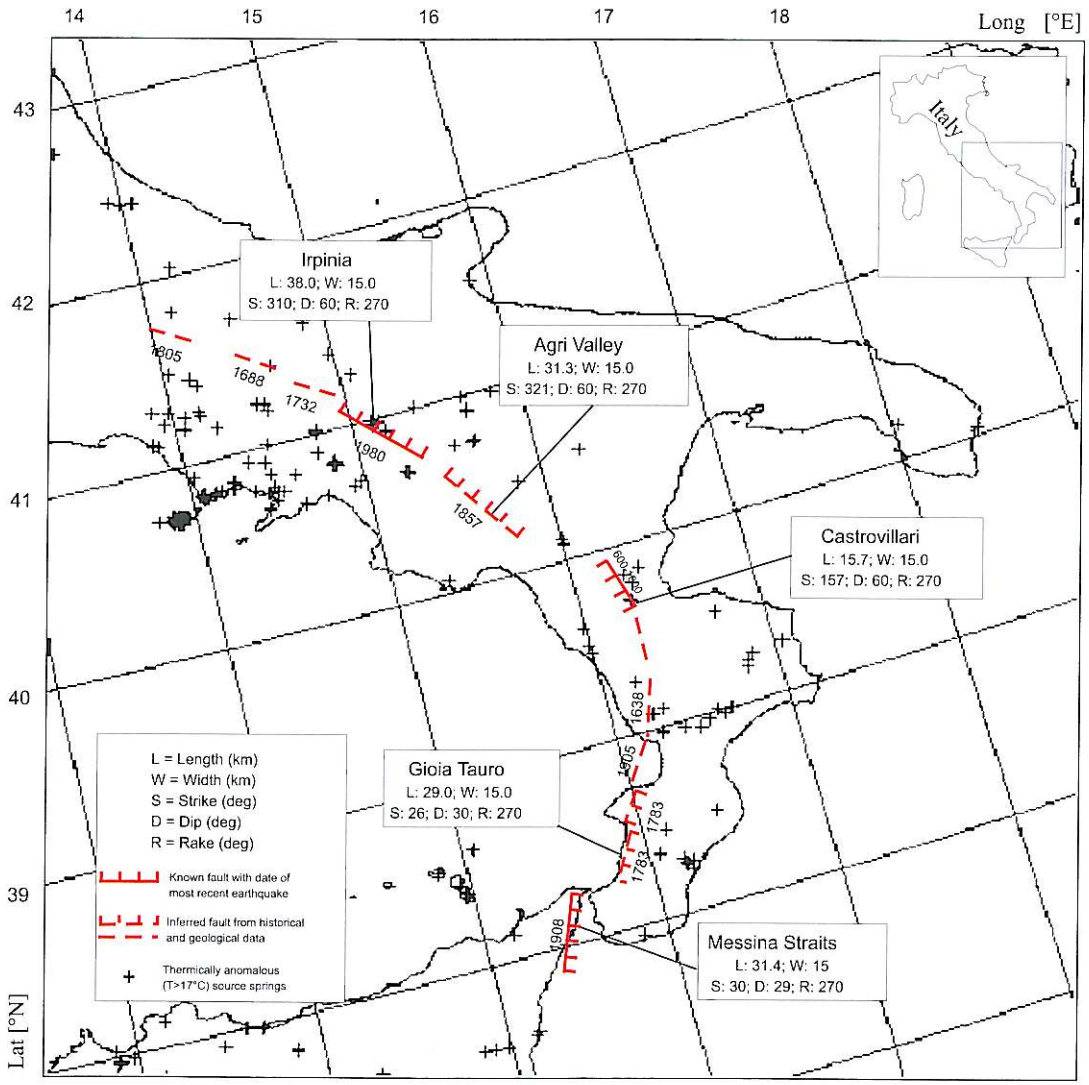

Fig. 1a. Study area: the main seismogenic faults (from Valensise *et al.*, 1993, http://faust.ingv.it/) and thermically anomalous ($T > 17$ °C) source springs as selected by Albarello and Martinelli (1997).

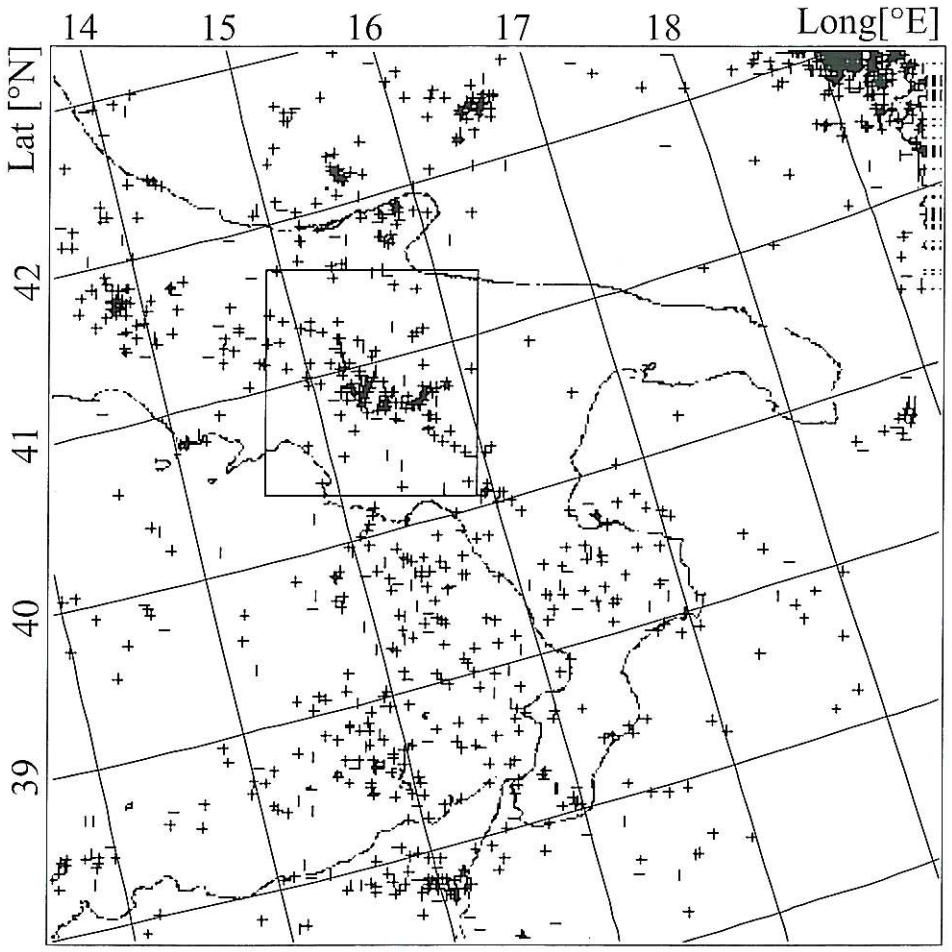

Fig. 1b. Study area: crosses indicate epicentre locations of earthquakes with magnitude $M_s > 3$ from 1963 to date as reported in the catalogue of the U.S. Council of the National Seismic System (CNSS). The box represents the area reported in figs. 4 and 5.

consistent energy release through significant aftershock sequences.

Another historically relevant event, the December 16, 1857 normal-faulting earthquake (Mallet, 1862), occurred in Val d'Agri. The seismic activity, which occurred in the study area after the 1980 event, consists of medium intensity earthquakes ($M_d \leq 5.0$, duration magnitude, as estimated by the seismometric network of National Institute of Geophysics) located close to the border between the Campania and Basilicata regions (Alessio *et al.*, 1995). The May 5, 1990 ($M_d = 5.0$) and May 26, 1991 ($M_d = 4.5$) earthquakes were the strongest events (Tertulliani *et al.*, 1992) to occur after the 1980 event. The seismological analysis of these events shows that they were generated by a strike-slip fault in the WE direction, perpendicular to the Apennine chain (Ekström, 1994; Boschi *et al.*, 1995). This fault lies north of the town of Potenza and is located between the two great seismogenic faults that caused the 1857 Val d'Agri earth-

quake to the south and the 1980 Irpinia earthquake to the north, respectively.

This area was chosen as test-area, and the Irpinia-Basilicata 1980 event as test case, mainly for the following reasons:

a) Together with one of the largest and well-documented events in the Italian peninsula, this area offers a seismic quiescence period long enough to permit the characterisation of the TIR signal in unperturbed conditions.

b) The area is also characterised by strong CO_2-dominated gas emissions (Doglioni *et al.*, 1996).

c) As part of an area of relatively recent orogenesis (lower Miocene - upper Pliocene-Pleistocene) characterised by a complex morphology and geology, it permits to better appreciate the performances of the proposed technique also in the less favourable conditions in terms of spatial homogeneity of ground elevation and spectral properties.

With reference to this test-area/event this study was carried out considering a quite extended area for which the following additional information was available:

1) Seismogenic faults as reported in the most recent studies (*e.g.*, Pantosti and Valensise, 1990; Valensise *et al.*, 1993; Boschi *et al.*, 1995, http://faust.ingv.it).

2) Locations of thermically anomalous ($T >$ 17°C) source springs (fig. 1a) as possible vehicle of greenhouse gases like CO_2 and CH_4 (hereafter simply source springs) selected by Albarello and Martinelli (1997).

3) Epicentres of earthquakes of magnitude $M_S > 3$ from 1963 to date (fig. 1b) as reported in the Catalogue of the U.S. Council of the National Seismic System (http://quake.geo.berkeley.edu/cnss/catalog-search.html/).

5. Results

Performances of the proposed approach were tested with reference to the strong earthquake (M_S = 6.9) which occurred in Southern Italy (Irpinia-Basilicata) on November 23, 1980 at 7.32 PM local time.

All NOAA/AVHRR satellite passes, collected in November, from 1994 to 1998, around 6.00 PM GMT (RAT prescriptions on the *temporal support T*), over the Southern Italian peninsula (RAT prescriptions on the *spatial support D*), were processed to build reference fields, (following steps from 1 to 5 described in Section 3). The mean $< \Delta T_4(\boldsymbol{r}) >$ and standard deviation $\sigma_{\Delta T4}(\boldsymbol{r})$ fields were computed for each location $\boldsymbol{r}$, and time-series $\Delta T_4(\boldsymbol{r}, t)$, (with $t \in$ T and $\boldsymbol{r} \in D$) deriving, for every year considered, the ALICE indexes, defined in (3.1) and (3.2).

In order to investigate a possible residual dependence on surface elevation and emissivity, indices (3.1) and (3.2) were co-located with the USGS GTOPO30 Digital Elevation Model (DEM) produced by the EROS Data Centre (with a ground resolution cell of about 1 km) and with a vegetation map (Normalized Difference Vegetation Index, NDVI) computed by means of the visible and near-infrared AVHRR channels 1 and 2. Results of the correlation analyses performed on the investigated area, shown in figs. 2 and 3 for November 1980, reveal a null dependence of the ALICE index $\otimes^{t}(\boldsymbol{r}, t')$ on both the elevation and the vegetation cover. The correlation coefficients, in both cases near to zero, assure, for such an index, a good protection by these natural noise sources. Residual observational noise, for example, from considering TIR radiances acquired from the same ground location under very different view-angles, as well as from errors in image-to-image co-location, are intrinsically taken into account in the standard deviation $\sigma_{\Delta T4}$. In this way, every residual «noisy» contribution to the TIR signal will contribute to increase the *llocal* value of $\sigma_{\Delta T4}$ reducing the corresponding ALICE values and probability of false anomalies.

By limiting our analysis only to the epicentral zone, the achieved results can be summarised as follows:

a) Figure 4 shows for the area around the epicentre (plotted together with its aftershocks) the average values of $\otimes^{S}(\boldsymbol{r}, t)$ computed for November 1980. Only pixels with $\otimes^{S}$ greater than 1.5 are depicted together with aftershock epicentres and source spring sites. From the picture it is easy to note how the epicentral zone and aftershocks alignments are well marked by higher values of $\otimes^{S}$. High values of $\otimes^{S}$ can also be observed in several zones away from the epicentral

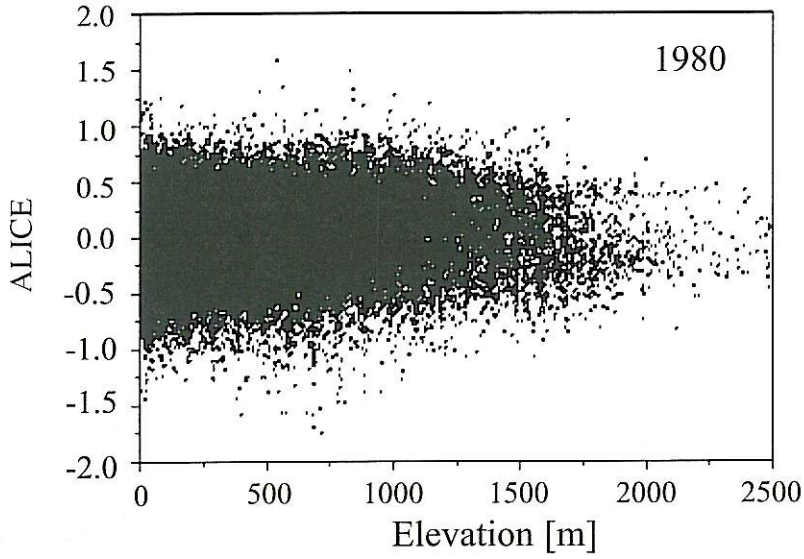

Fig. 2. Correlation analysis between the average ALICE index $\otimes'(r,t)$ and the elevation for the study area in November 1980 (see text).

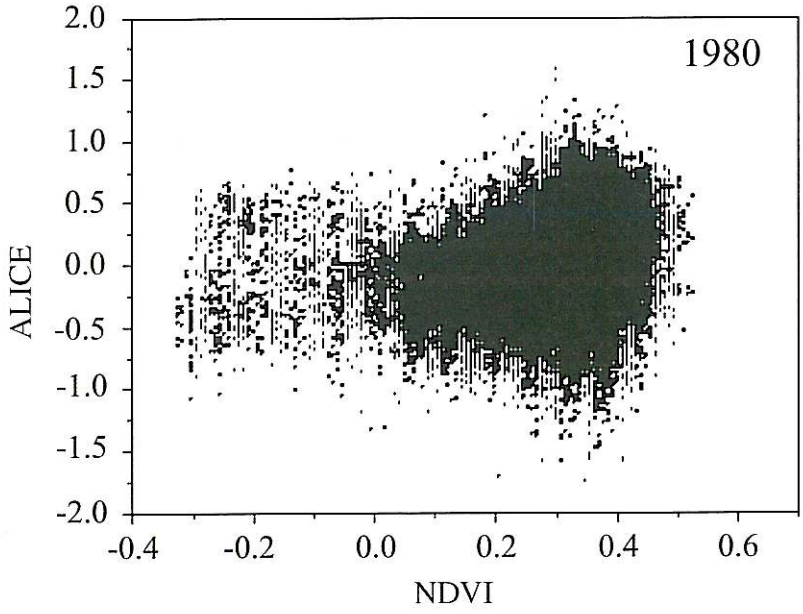

Fig. 3. Correlation analysis between the average ALICE index $\otimes'(r,t)$ and the vegetation index (NDVI) for the study area in November 1980 (see text).

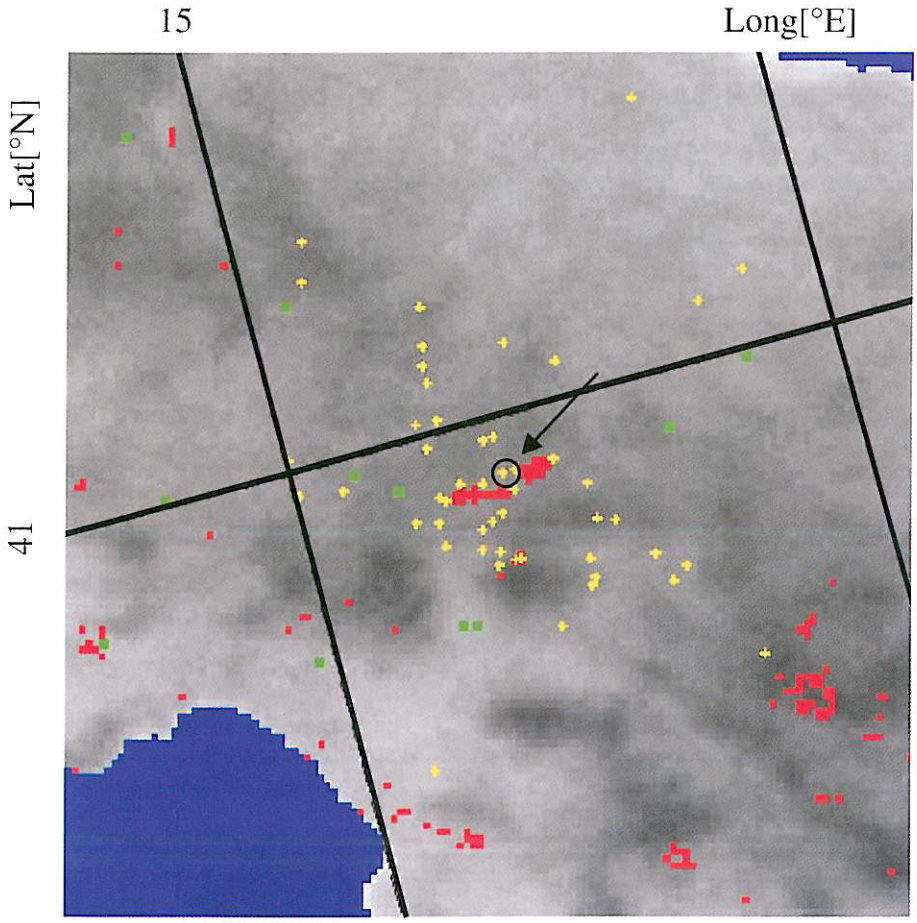

Fig. 4. Irpinia-Basilicata earthquake ($M_s = 6.9$, November 23, 1980, 7.32 PM): spatial distribution of the average ALICE index $\otimes^s(\boldsymbol{r}, t')$ over the area around the epicentre (circled) for November 1980. Yellow crosses indicate aftershocks position; green symbols localise spring sources. Pixels with $\otimes^s > 1.5$ are depicted in red. In the background the reference field $<\Delta T_4(\boldsymbol{r}')>$ (see text) is depicted in grey tones (from dark to bright).

zone. By comparison with figs. 1a and 1b it is easy to see how they are well related to seismically active areas and/or source spring sites.

b) The average values of $\otimes^t(\boldsymbol{r}, t)$ were computed for November 1980. They are generally lower and well within the present natural/observational noise level. In fig. 5 only pixels with $\otimes^t$ values higher than 0.6 are depicted together with aftershock epicentres and source spring sites. They still result in good correlation with the epicentral zone and aftershock alignments and, as in the previous case, when observed away from the epicentral zone, they are well related to seismically active areas and/or source spring sites (see figs. 1a and 1b by comparison).

c) Figure 6 shows the temporal evolution of the area (measured in AVHRR pixels) with $\otimes^t$ values greater than 0.6 in a circle of 100 km of radius around the epicentre, a few days before and after the earthquake. Even though temporal gaps are present (only AVHRR imagery free of clouds on the area have been used), it is never-

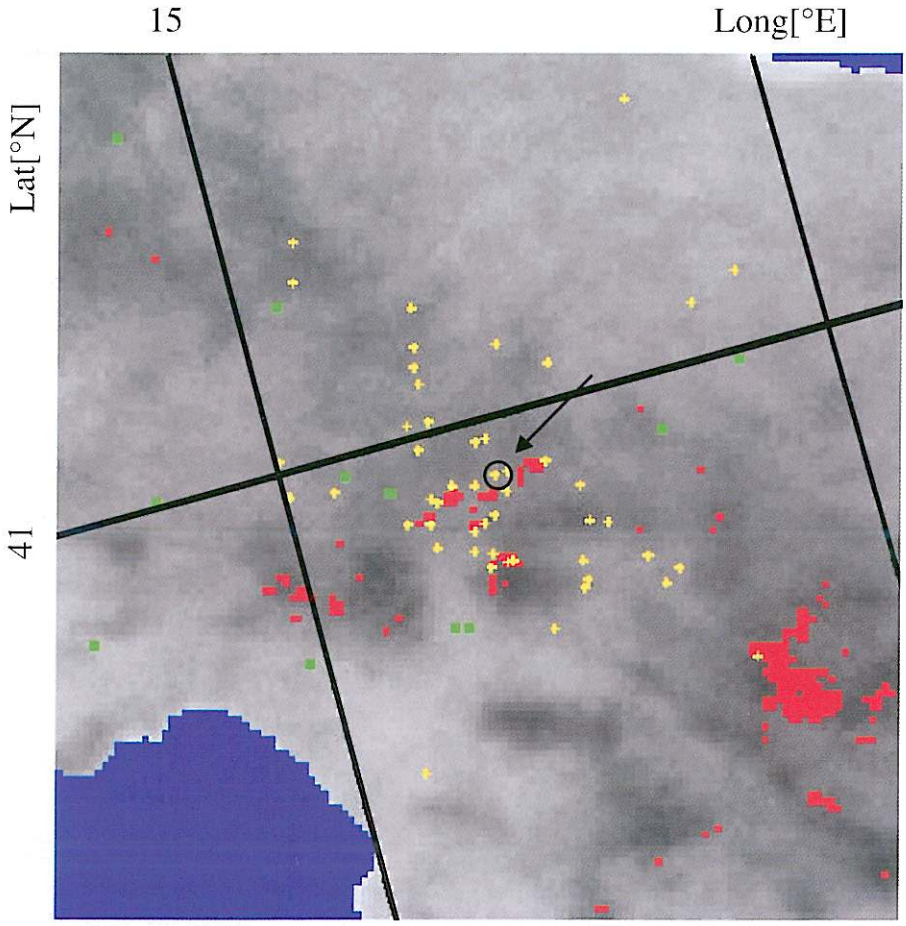

Fig. 5. As fig. 4 for the ALICE index $\otimes^{t}(\boldsymbol{r},t)$. Pixels with $\otimes^{t} > 0.6$ are depicted in red.

theless possible to appreciate the doubling of the extension of the over-threshold area from November 16 and 20 with a further outstanding increase during the following three days preceding the earthquake.

By extending our analysis all over the investigated area (depicted in fig. 1a,b), we achieved the following results:

d) Figure 7 represents an extended view of fig. 5, showing the average values of $\otimes^{t}(\boldsymbol{r},t)$ computed for November 1980 (only pixels with values higher than 0.6 are depicted). It is possible to note how over-threshold pixels can also be observed far away (up to several hundred kilometres) from the epicentral zone. Figures 8 and 9 refer, respectively, to the relatively *unperturbed* cases of November 1994 and November 1998 for which only a few events with $M_S > 3$ (no one with $M_S > 4$) can be found in published catalogues. By comparison, it is easy to recognise how the extension of over-threshold areas is incomparably higher during November 1980.

e) Figure 10 shows the temporal evolution of the percentage, with respect to their number all over the investigated area, of the over-threshold pixels within a circle of 100 km of radius around the epicentre a few days before and after

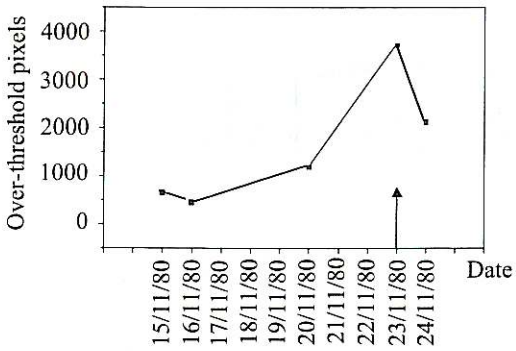

Fig. 6. Irpinia-Basilicata earthquake (M_s = 6.9, November 23, 1980, 7.32 PM): temporal evolution of the extension of the over-threshold area around the epicentre. The number of pixels with $\otimes' > 0.6$, in a circle of 100 km of radius around the epicentre, is plotted a few days before and after the earthquake occurrence (black arrow).

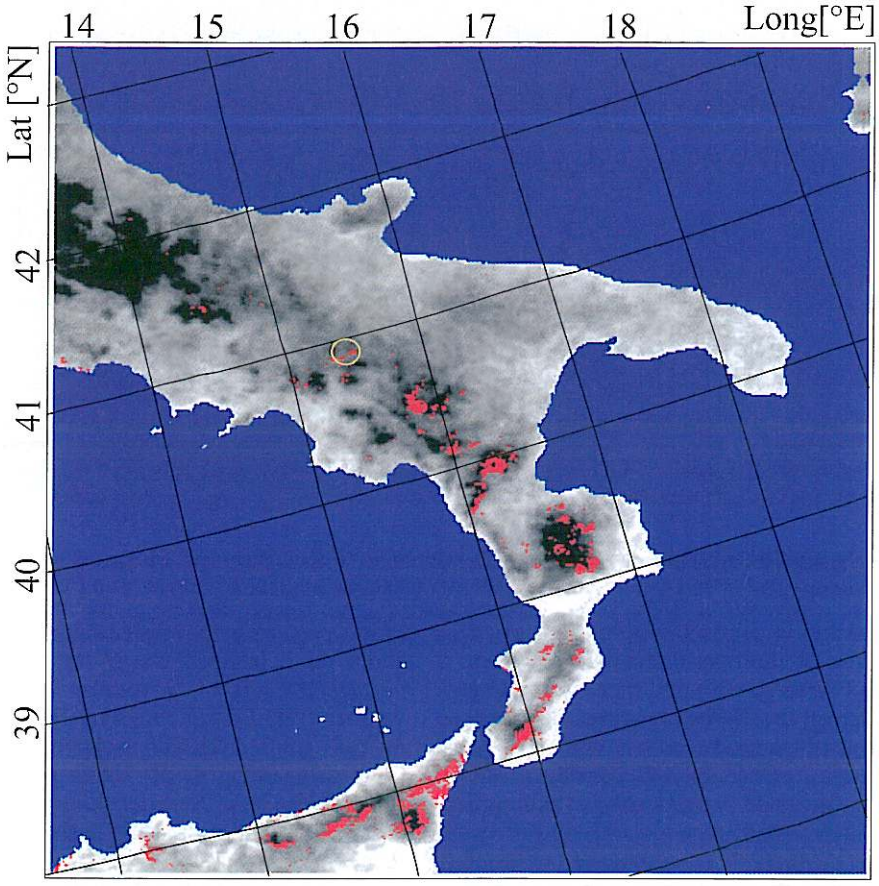

Fig. 7. Irpinia-Basilicata earthquake (M_s = 6.9, November 23, 1980, 7.32 PM): spatial distribution of the average ALICE index $\otimes'(r,t)$ over the whole study area for November 1980. Pixels with $\otimes' > 0.6$ are depicted in red. The yellow circle represents the epicentral zone. In the background the reference field $<\Delta T_4(r')>$ (see text) is depicted in grey tones (from dark to bright).

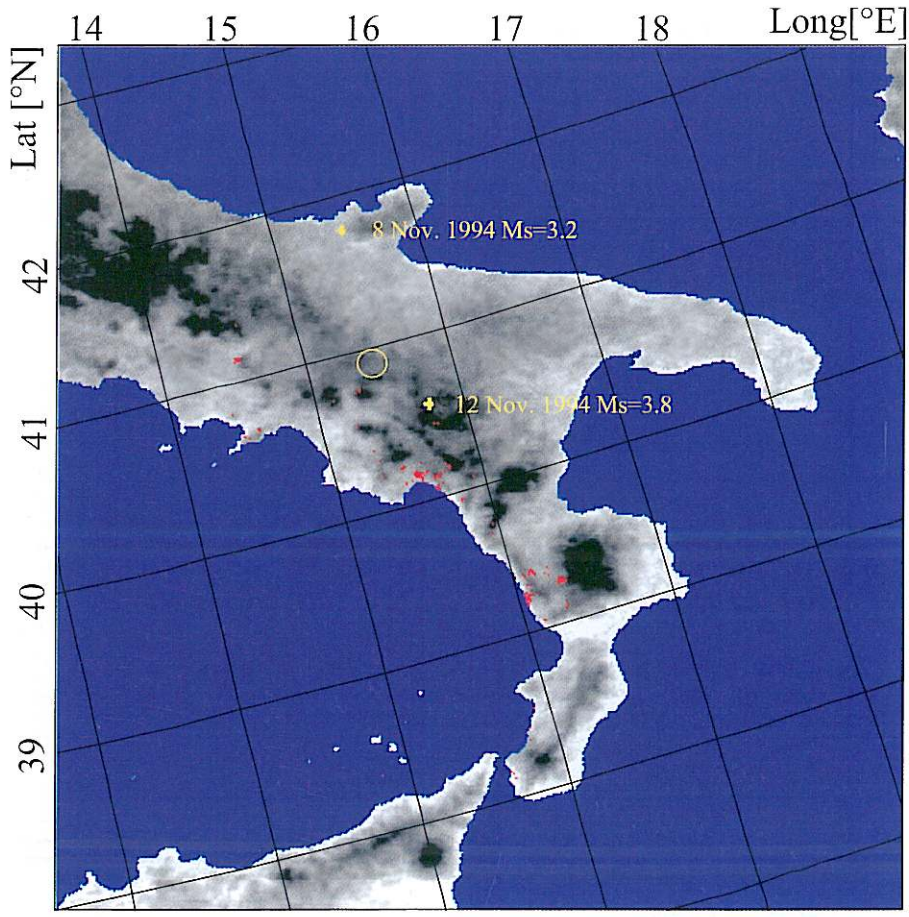

Fig. 8. As fig. 7 for November 1994. The yellow crosses indicate the location of the two events with $M_S > 3$ in the area during November 1994.

the 23 November 1980 Irpinia-Basilicata earthquake. It is remarkable that the number of over-threshold pixels in the epicentral area, representing no more than 10% of the total on November 16, passes suddenly to a value higher than 40% on November 20, maintaining such high values also on the following days. This suggests that the process of extension of the over-threshold area was particularly intense in the epicentral zone a few days before the earthquake.

f) In order to understand whether or not the spatial distribution of the over-threshold pixels reported in fig. 8 can be put in some relation with seismogenic areas, the following analysis was performed:

– Seismogenic faults (694 pixels on the scene) and source spring sites (167 in the scene) reported in fig. 1a as well as epicentres of earthquakes of magnitude $M_S > 3$ from 1963 to date (1834 on the scene) reported in fig. 1b, were all considered possible indicators of seismically active zones and a possible location of greenhouse gas discharge.

– For each over-threshold pixel in fig. 7, the distance from the closest of these indicators (and separately for each typology) was computed. The

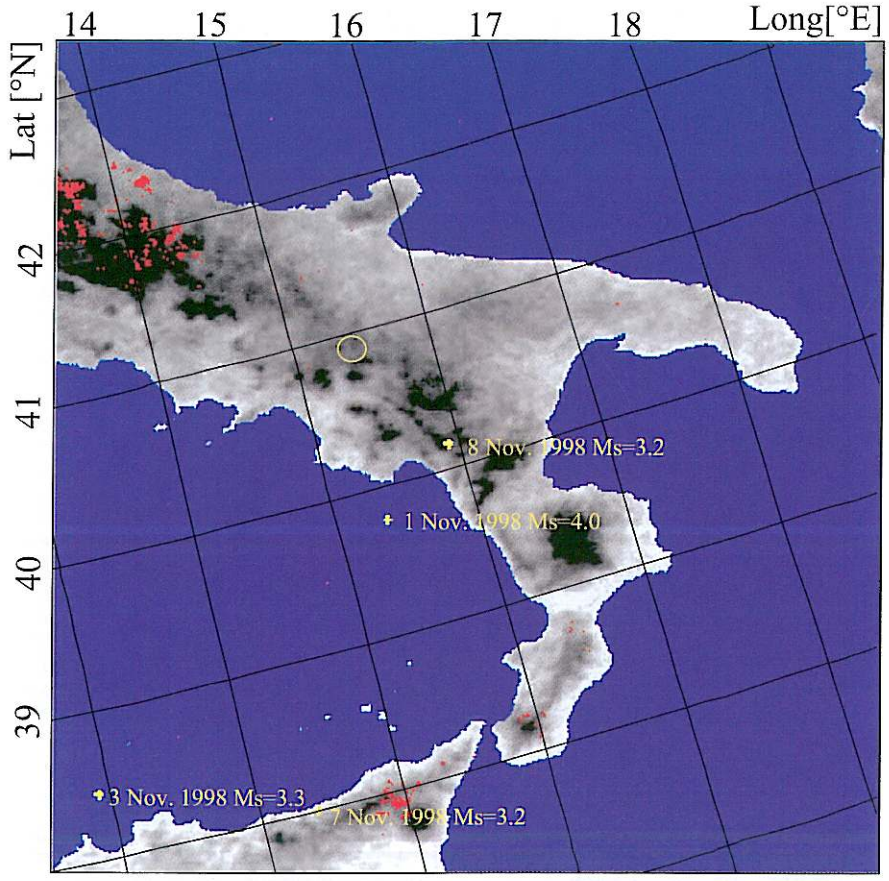

Fig. 9. As fig. 7 for November 1998.

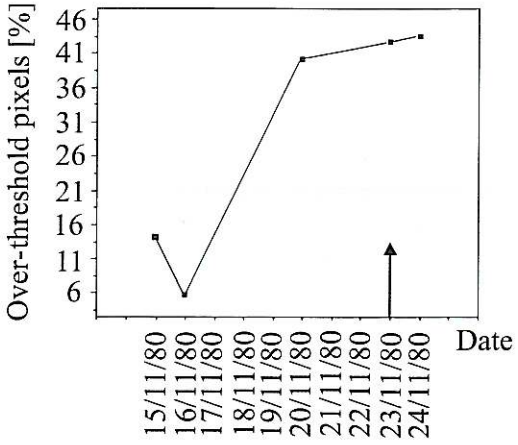

Fig. 10. Irpinia-Basilicata earthquake (M_s = 6.9, November 23, 1980, 7.32 PM): comparative analysis of the temporal evolution of the extension of the over-threshold areas within and far away from the epicentral zone. The percentage of pixels (over the total with $\otimes' > 0.6$) falling in a circle of 100 km of radius around the epicentre, is plotted a few days before and after the earthquake occurrence (black arrow).

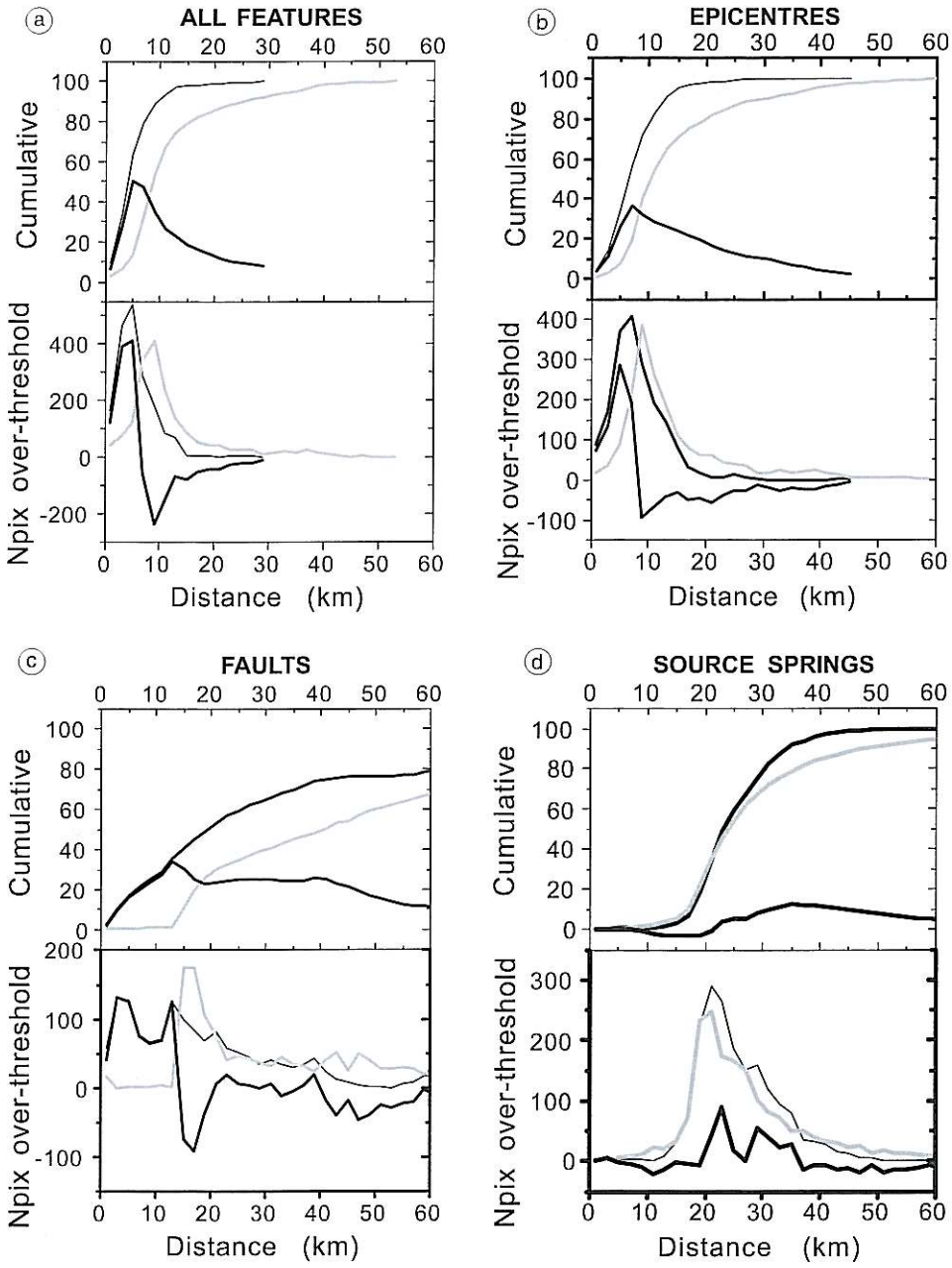

Fig. 11a-d. November 1980: comparative correlation analysis between the actual spatial distribution of over-threshold pixels and a synthetic set (with the same average density) of randomly distributed points, together with the seismogenic indicators over the whole study area (see text): a) all features; b) epicentres; c) faults; d) source springs. Top: cumulative distribution; bottom: histogram. For all cases the actual data (thin black), the synthetic set (thick, light grey) and their difference (thick black) are shown.

same analysis was performed using a synthetic random distribution of over-threshold pixels having the same spatial density across the scene.

– The histograms and cumulative distributions of the number of over-threshold pixels (resulting from both the actual and random distribution) *versus* distance were computed and plotted together in fig. 11a-d.

From fig. 11a it is possible to note that more than 95% of the over-threshold pixels are less than 10 km from whatever indicator and quite all of them at less than 15 km. The spatial distribution of over-threshold pixels appears (fig. 11b) particularly related to epicentres (with a modal value around 7 km and a 90% of probability to find over-threshold pixels at less than 12 km from an epicentre) and less related (fig. 11c) to seismogenic faults distribution. Thermically anomalous ($T > 17$°C) source springs (Albarello and Martinelli, 1997) appear (fig. 11d) systematically shifted with respect to over-threshold pixels whose spatial distribution has a modal value around 20 km with more than a 90% probability of finding them between 20 and 40 km away from the closest spring source. Comparing actual and simulated distributions, it is possible to note how the observed spatial correlation with over-threshold pixels is not fortuitous in the case of epicentres (that give the main contribution to the overall correlation) and, as far as distances shorter than 20 km are concerned, in the case of seismogenic faults. On the other hand, fig. 11d clearly indicates the absence of correlation between over-threshold pixels and source spring sites distribution.

6. Discussion

The main target of this work was to devise a new approach to satellite TIR survey for seismogenic regions monitoring. The RAT approach (Tramutoli, 1998) has been applied in a simplified form mainly aiming at a preliminary estimate of the TIR signal-to-noise ratio in the worst informative context. In particular, only the most simple natural and observational noise sources have been removed both in the temporal and spatial domain, avoiding, at this preliminary stage, the use of any specific model to achieve a further noise level reduction. Results achieved in the case-study of the Irpinia-Basilicata earthquake of November 23, 1980 ($M_s = 6.9$) show how the observed TIR excesses (defined by $\otimes^t(r,t)$ in the temporal domain) still remain within the noise level so that a refined noise-removal approach should be applied to reduce the residual natural and observational noise to a statistically acceptable level. Major improvements in this direction can be expected by the use of more refined cloud/snow detection techniques (*e.g.*, following Derrien *et al.*, 1993) and by the introduction of standard corrections taking into account the *llocal* variability of atmospheric water vapour content and satellite view angle. At this preliminary stage, we understood that, at least in the time domain (and especially when averaged on a monthly basis as in our case), we are dealing with a very weak *llocal* signal.

Signal-to-noise ratios higher than 1.5 (open to further improvements as in the previous case) have been achieved for $\otimes^s(r,t)$ after the analysis performed in the spatial domain.

Even with the above-mentioned limitations, the temporal evolution of the areas with higher TIR excesses appears in some relation with the seismogenic areas distribution and their activation in the case study considered. Also by comparison with the results of the analyses performed on relatively *unperturbed* years, which do not show similar effects, it appears that the observed TIR excesses extend their presence far away (several hundred of kilometres) from the epicentral zone and with a non casual spatial correlation with seismoactive regions marked by the epicentres of recent earthquakes of magnitude $M_s > 3$.

A number of indications emerge from this preliminary study:

a) It seems to confirm, even in a more complex context and using a completely different methodology, the indications from the work of Tronin (1996) who found a correlation between seismic areas activation and the widening of TIR anomalies.

b) It suggests, in the case study of the Irpinia-Basilicata earthquake, the possible presence of large scale (up to several hundred kilometres)

effects up to now not otherwise documented even if perfectly compatible with theoretical considerations (*e.g.*, Dobrovolsky *et al.*, 1979; Fleisher, 1981) and observational evidence related to events of similar magnitude in other geographic areas (Qiang Zu-ji *et al.*, 1992b).

c) The observed spatial distribution of over-threshold pixels with respect to thermally anomalous spring sources raises several problems (mainly on the spatial distribution and change with the time of gas emissions) to be better investigated, also in the light of recent studies performed in the same area by Martinelli *et al.* (1999) – indicating a systematic shift between thermal springs and seismogenic faults distribution – and Italiano *et al.* (2000) who found a substantial stability with the time (no quick discharge) of gas emission due to the most important spring sources considered in this paper. The poor correlation found in this case, in comparison with the high correlation achieved using epicentres or, to a lesser extent, seismogenic faults, might indicate (if the claimed origin of TIR anomalies from a localised greenhouse effect is confirmed by further specific studies) a major role to be attributed to occasional rather than permanent gas discharges in the context of seismogenic areas monitoring activities.

Acknowledgements

This work was carried out within the framework of «Pollino» (POP-FESR 1993-1996) and «TIMORAN» (POP-FESR 1994-1999) Projects, both jointly funded by the European Economic Community and Regione Basilicata. The authors thank R. Console for closely and accurately reviewing the earlier version of the manuscript improving its clarity and completeness. The authors are also indebted to G. Martinelli who warmly encouraged the start of this work sharing time and knowledge in very useful discussions.

REFERENCES

ALBARELLO, D. and G. MARTINELLI (1997): Main constraints for siting monitoring networks devoted to the study of earthquake related hydrogeochemical phenomena in Italy, *Ann. Geofis.*, **40** (6), 1505-1525.

ALESSIO, G., F. ESPOSITO, A. GORINI and S. PORFIDO (1995): Detailed study of the Potentino seismic zone in the Southern Apennines, *Tectonophysics*, **250**, 113-134.

AMATO, A. and G. SELVAGGI (1993): Aftershock location and *P*-velocity structure in the epicentral region of the 1980 Irpinia earthquake, *Ann. Geofis.*, **36** (1), 3-15.

BECKER, F. (1987): The impact of spectral emissivity on the measurement of land surface temperature from a satellite, *Int. J. Remote Sensing*, **8**, 1509-1522.

BERNARD, P. and A. ZOLLO (1989): The Irpinia 1980 earthquake: detailed analysis of a complex normal faulting, *J. Geophys. Res.*, **94**, 1631-1647.

BOSCHI, E., G. FERRARI, P. GASPERINI, E. GUIDOBONI, G. SMRIGLIO and G. VALENSISE (Editors) (1995): *Catalogo dei Forti Terremoti in Italia dal 461 a.C. al 1980* (ING, Roma – SGA, Bologna), pp. 974.

DERRIEN, M., B. FARKI, L. HARANG, H. LE GLEAU, A. NOYALET, D. POCHIC and A. SAIROUNI (1993): Automatic cloud detection applied to NOAA-11/AVHRR imagery, *Remote Sensing Environ.*, **46**, 246-267.

DOBROVOLSKY, I.P., S.I. ZUBKOV and V.I. MIACHKIN (1979): Estimation of the size of earthquake preparation zones, *Pageoph*, **117**, 1025-1044.

DOGLIONI, C., P. HARABAGLIA, G. MARTINELLI, F. MONGELLI and G. ZITO (1996): A geodynamic model of the Southern Apennines accretionary prism, *Terra Nova*, **8**, 540-547.

EKSTRÖM, G. (1994): Teleseismic analysis of the 1990 and 1991 earthquakes near Potenza, *Ann. Geofis.*, **37** (6), 1591-1599.

FLEISCHER, R.L. (1981): Dislocation model for radon response to distant earthquakes, *Geophys. Res. Lett.*, **8** (3), 477-480.

IRWIN, W.P. and BARNES, I. (1980): Tectonic relations of carbon dioxide discharges and earthquakes, *J. Geophys. Res.*, **85**, 3115-3121.

ITALIANO, F., M. MARTELLI, G. MARTINELLI and P. MARIO NUCCIO (2000): Geochemical evidence of melt intrusion along lithospheric faults of the Southern Apennines, Italy: geodynamic and seismogenic implications, *J. Geophys. Res.*, **105**, 13569-13578.

LAURITSON, L., G.J. NELSON and F.W. PORTO (1979): Data extraction and calibration of TIROS-N/NOAA radiometers, *NOAA Technical Memorandum NESS 107*, U.S. Department of Commerce, Washington, D.C., U.S.A.

MALLET, R. (1862): *Great Neapolitan Earthquake of 1857. The First Principles of Observational Seismology*, London, 1862, Reprinted by ING-SGA Bologna, pp. 862 (1987).

MARTINELLI, G., M. MUCCIARELLI and G. VALENSISE (1999): Relationship between the location of thermal springs and seismogenic faults in the Apennines, Italy, in *Proceedings of the European Geophysical Society, XXIV General Assembly, The Hague, 19-23 April 1999*, p. 99.

PANTOSTI, D. and G. VALENSISE (1990): Faulting mechanism and complexity of the November 23, 1980, Campania Lucania earthquake, inferred from surface observations, *J. Geophys. Res.*, **95**, 15329-15341.

PERGOLA, N. and V. TRAMUTOLI (2000): SANA: Sub-pixel Automatic Navigation of AVHRR imagery, *Int. J. Remote Sensing Lett.*, **21** (12), 2519-2524.

QIANG ZU-JI, XU XIU-DENG and DIAN CHANG-GONG (1991): Thermal infrared anomaly – precursor of impending earthquakes, *Chin. Sci. Bull.*, **36** (4), 319-323.

QIANG ZU-JI, DIAN CHANG-GONG, WANG XUAN-JI and HU SI-YI (1992a): Satellite thermal infrared anomalous temperature increase and impending earthquake precursor, *Chin. Sci. Bull.*, **37** (19), 1642-1646.

QIANG ZU-JI and DIAN CHANG-GONG (1992b): Satellite thermal infrared impending temperature increase precursor of Gonghe earthquake of magnitude 7.0, Qinghai province, *Geoscience*, **6** (3), 297-300.

SCHOLZ, C.H., L.R. SYKES and Y.P. AGGARWAL (1973): Earthquake prediction: a physical basis, *Science*, **181**, 803-810.

TERTULLIANI, A., M. ANZIDEI, A. MARAMAI, M. MURRU and F. RIGUZZI (1992): Macroseismic study of the Potenza (Southern Italy) earthquake of 5 May 1990, *Natural Hazards*, **6**, 25-38.

TRAMUTOLI, V. (1998): Robust AVHRR Techniques (RAT) for environmental monitoring: theory and applications, in *Earth Surface Remote Sensing II*, edited by G. CECCHI and E. ZILIOLI, *SPIE 3496*, 101-113.

TRONIN, A.A. (1996): Satellite thermal survey – a new tool for the study of seismoactive regions, *Int. J. Remote Sensing*, **17** (8), 1439-1455.

VALENSISE, G., D. PANTOSTI, G. D'ADDEZIO, F.R. CINTI and L. CUCCI (1993): L'identificazione e la caratterizzazione di faglie sismogenetiche nell'Appennino centro-meridionale e nell'arco calabro: nuovi risultati e ipotesi interpretative, in *Proceedings of the GNGTS-CNR Annual Meeting*, Rome, 331-342.

WANG, L. and C. ZHU (1984): Anomalous variations of ground temperature before the Tangsan and Haiheng earthquakes, *J. Seismological Res.*, **7**, 649-656.

WESTAWAY, R. and J. JACKSON (1987): The earthquake of 1980 November 23 in Campania Basilicata (Southern Italy), *Geophys. J. R. Astron. Soc.*, **90**, 375-443.